New Phytologist

The BIG protein distinguishes the process of CO2-induced stomatal closure from the inhibition of stomatal opening by CO2.

Journal:	*New Phytologist*
Manuscript ID	NPH-MS-2017-24821.R1
Manuscript Type:	MS - Regular Manuscript
Date Submitted by the Author:	n/a

Complete List of Authors:	He, Jingjing; Wuhan University, Department of Plant Sciences Zhang, Rouxi; Wuhan University, Department of Plant Sciences Peng, Kai; University of Bristol, Biological Sciences Tagliavia, Cecilia; Lancaster University, Lancaster Environment Centre Li, Siwen; Wuhan University, Department of Plant Sciences Xue, Shaowu; Huazhong Agricultural University, College of Life Science and Technology Liu, Amy; University of California at San Diego, Cell and Developmental Biology Section, Division of Biological Sciences Hu, Honghong; Huazhong Agricultural University, College of Life Science Zhang, Jingbo; University of California, San Diego, Division of Biology Hubbard, Katherine; University of Hull, School of Environmental Sciences Held, Katrin; Universität Münster, Institut für Biologie und Biotechnologie der Pflanzen McAinsh, Martin; Lancaster University, Department of Biological Sciences Gray, Julie; University of Sheffield, Molecular Biology & Biotechnology Kudla, Jörg; Universität Münster, Institut für Botanik und Botanischer Garten Schroeder, Julian; University of California, San Diego, Division of Biology Liang, Yun-Kuan; Wuhan University, Department of Plant Sciences Hetherington, Alistair; University of Bristol, School of Biological Sciences

Key Words:	Abscisic acid, BIG gene, CO2 signalling, Stomatal function, S-type anion channel

Title: The BIG protein distinguishes the process of CO_2-induced stomatal closure from the inhibition of stomatal opening by CO_2.

Jingjing He[1,#], Ruo-Xi Zhang[1,#], Kai Peng[2], Cecilia Tagliavia[3], Siwen Li[1], Shaowu Xue[4], Amy Liu[5], Honghong Hu[4,5], Jingbo Zhang[5], Katherine E Hubbard[5,6], Katrin Held[7], Martin R McAinsh[3], Julie E Gray[8], Jörg Kudla[7], Julian I Schroeder[5], Yun-Kuan Liang[1]* and Alistair M Hetherington[2]*

[1]State Key Laboratory of Hybrid Rice, Department of Plant Sciences, College of Life Sciences, Wuhan University, Wuhan 430072, China

[2]School of Biological Sciences, Life Sciences Building, 24 Tyndall Avenue, Bristol BS8 1TQ, UK

[3]Lancaster Environment Centre, Lancaster University, Lancaster, LA1 4YQ, UK

[4]College of Life Science and Technology, Huazhong Agricultural University, Wuhan 430070, China

[5]Cell and Developmental Biology Section, Division of Biological Sciences, University of California at San Diego, La Jolla, California 92093, USA

[6]School of Environmental Sciences, University of Hull, HU6 7RX, UK.

[7]Institut für Biologie und Biotechnologie der Pflanzen, Universität Münster, Schlossplatz 7, Münster 48149, Germany

[8]Department of Molecular Biology and Biotechnology, University of Sheffield, Firth Court, Western Bank, Sheffield, S10 2TN, UK

[#]These authors contributed equally to this work.

* Authors for correspondence:

Yun-Kuan Liang (ORCID ID 0000-0001-5869-5931), Tel. +86 27 68752363

Email: ykliang@whu.edu.cn

Alistair M Hetherington (ORCID ID 0000-0001-6060-9203), Tel. +44 117 3941188

Email: Alistair.Hetherington@bristol.ac.uk

Total word count:

Title: 18

Summary: 194

Main text (Introduction, Materials and Methods, Results, Discussion, and Acknowledgements): 4672

Introduction: 915

Results: 1436

Discussion: 1051

Materials and Methods: 1144

Acknowledgements: 124

Number of Figures: 5

Supplemental Figures: 3

Supplemental Text: 1

Summary

- We conducted an infrared thermal imaging-based genetic screen to identify Arabidopsis mutants displaying aberrant stomatal behavior in response to elevated concentrations of CO_2.
- This approach resulted in the isolation of a novel allele of the Arabidopsis *BIG* locus (*At3g02260*) that we have called *cis1* (for ***C**O$_2$ **i**nsensitive **1***).
- *BIG* mutants are compromised in elevated CO_2-induced stomatal closure and bicarbonate activation of S-type anion channel currents. In contrast to wild type they fail to exhibit reductions in stomatal density and index when grown in elevated CO_2. However, like wild type, *BIG* mutants display inhibition of stomatal opening when exposed to elevated CO_2. *BIG* mutants also display wild type stomatal aperture responses to the closure-inducing stimulus ABA.
- Our results indicate that BIG is a signaling component involved in the elevated CO_2-mediated control of stomatal development. In the control of stomatal aperture by CO_2, BIG is only required in elevated CO_2-induced closure and not in the inhibition of stomatal by this environmental signal. These data show that, at the molecular level, the CO_2 mediated inhibition of opening and promotion of stomatal closure signalling pathways are separable and BIG represents a distinguishing element in these two CO_2-mediated responses.

Key words: Abscisic acid, *BIG* gene, CO_2 signalling, Stomatal function, S-type anion channel

Introduction

Stomata consist of a pair of guard cells that surround a central pore and serve to regulate water loss and the uptake of CO_2. Both the aperture of the stomatal pore and the number of stomata that develop on the leaf surface are controlled by environmental signals. By integrating external signals and local cues stomata "set" gas exchange to suit the prevailing environmental conditions (Hetherington & Woodward, 2003). One of the signals that controls stomatal aperture and influences stomatal development, in both the short and long term, is the atmospheric concentration of carbon dioxide ($[CO_2]$) (Kim *et al.*, 2010; Franks *et al.*, 2012). In response to an increase in $[CO_2]$ stomatal aperture reduces, as in general, do the number of stomata that develop on the surface of leaves (Vavasseur & Raghavendra, 2005; Kim *et al.*, 2010; Franks *et al.*, 2012). Understanding how the plant perceives changes in $[CO_2]$ and integrates this information with other internal and external signals, resulting in the adjustments of stomatal aperture and density is of key importance in the context of understanding the impact of global environment change on plants (Assmann & Jergla, 2016).

Recently we have begun to understand more about the underlying cellular mechanisms responsible for coupling increased $[CO_2]$ to reduced stomatal conductance (Kim *et al.*, 2010; Assmann & Jergla, 2016; Engineer *et al.*, 2016). In this context it is important to recognize that elevated CO_2-induced reductions in stomatal conductance are the net result of two processes: these are the promotion of stomatal closure and the inhibition of stomatal opening (Assmann, 1993). These processes are separable; ABA induced-stomatal closure is distinct from ABA inhibited-stomatal opening (Allen *et al.*, 1999; Wang *et al.*, 2001; Mishra *et al.*, 2006). However, prior to the current work it was not known whether this also applied to $[CO_2]$-induced changes in stomatal aperture.

There is evidence that the guard cell ABA and CO_2 signaling responsible for the inhibition of light-induced stomatal opening pathways converge (Webb & Hetherington, 1997). It has been suggested that elevated [CO_2] brings about its effects on stomatal aperture and development by accessing the ABA signaling pathway because there is a requirement for both ABA and the ABA receptors of the PYR/RCAR family in these responses (Chater *et al.*, 2015). There are other data suggesting that the early steps in CO_2-mediated closure converge with ABA signaling downstream of ABA receptors and the two pathways influence each other upon convergence (Xue *et al.*, 2011; Merilo *et al.*, 2013; Horak *et al.*, 2016; Jakobson *et al.*, 2016; Yamamoto *et al.*, 2016). Obviously, these processes are not mutually exclusive. Although the mechanism(s) through which the guard cell ABA signaling pathway is accessed is not fully understood, it has been possible to distinguish, on a genetic basis, components that function in CO_2 mediated closure but not in guard cell ABA signaling. In *Arabidopsis* these include β-carbonic anhydrases which are encoded by the *CA1* and *CA4* genes (Hu *et al.*, 2010), the protein kinase HT1 (HIGH LEAF TEMPERATURE 1) (Hashimoto *et al.*, 2006), RHC1, a MATE transporter (Tian *et al.*, 2015) and the MAP kinase MPK4 (Horak *et al.*, 2016; Jakobson *et al.*, 2016). Loss of the CAs, RHC1, MPK4 impairs CO_2-induced closure (Hashimoto *et al.*, 2006; Hu *et al.*, 2010; Tian *et al.*, 2015; Horak *et al.*, 2016; Jacobsen *et al.*, 2016) whereas recessive *ht1* alleles show a constitutive high CO_2 response (Hashimoto *et al.*, 2006; Hashimoto-Sugimoto *et al.*, 2016).

In 1987, Woodward discovered an inverse relationship between atmospheric [CO_2] and stomatal density (Woodward, 1987). We know less about the operation of this developmental signaling pathway, however, the putative β-keto acyl CoA synthase encoded by the *HIC* gene is involved as are the **C**O_2 **R**esponse **S**ecreted **P**rotease (CRSP), the β-carbonic anhydrases CA1 and CA4 and the peptide, Epidermal Patterning Factor 2 (EPF2) (Gray *et al.*, 2000; Doheny-Adams *et al.*, 2012; Engineer

et al., 2014). Most recently, it has been shown that the activity of the ROS producing NADPH oxidases encoded by the *RBOHD* and *RBOHF* genes are involved in the CO_2-mediated reduction in stomatal density as is ABA and the ABA receptors encoded by the PYR/RCAR family (Chater *et al.*, 2015).

During an infrared thermal imaging genetic screen in Arabidopsis (Wang *et al.*, 2004) we isolated a novel allele of the *BIG* locus（*At3g02260*） that we name *cis1* (for ***C****O*$_2$ ***i****n****s****ensitive **1***) that is compromised in both elevated [CO_2]-induced closure and reduction in stomatal density. However, when challenged with ABA *cis1* displays reductions in stomatal aperture that are indistinguishable from WT suggesting that *BIG* (*CIS1*) functions upstream of ABA or in an ABA-independent signaling pathway responsible for the control of stomatal aperture by CO_2. We also found that activation of the guard cell S-type anion channel by bicarbonate is compromised by the loss of *BIG* function. Furthermore, in contrast to elevated [CO_2]-mediated closure, the ability of elevated [CO_2] to inhibit stomatal opening was not affected in this mutant. In summary, we have identified BIG as a new component in the signaling pathway responsible for the control of stomatal development by elevated [CO_2]. We also show that *BIG* also features in the signaling pathway through which elevated [CO_2] controls stomatal aperture. Importantly, we show that BIG is only involved in elevated [CO_2]-induced stomatal closure and is not involved in the inhibition of stomatal opening by this environmental signal or in stomatal responses to ABA. These results show that, at the molecular level, these pathways are separable, with BIG representing a component that distinguishes these two CO_2-mediated responses.

Results

The *cis1* mutant is involved in the response of stomatal conductance to elevated CO_2.

To understand the underlying cellular basis of the effect of elevated CO_2 on stomatal development and function we carried out a forward genetic screen using infrared thermography. We reasoned that mutants failing to exhibit reductions in aperture, in this case induced by exposure to elevated [CO_2], would be visible because they would exhibit reduced leaf temperature due to increased leaf evapotranspiration relative to WT (Darwin, 1904). Infrared thermography has been used previously to isolate mutants carrying lesions in stomatal responses to ABA (Raskin & Ladyman 1988; Merlot *et al.*, 2002), reduced atmospheric relative humidity (Xie *et al.*, 2006; Liang *et al.*, 2010) and CO_2 (Hashimoto *et al.*, 2006; Negi *et al.*, 2008). Using this approach we screened M2 plants from an EMS-mutagenized population of *Arabidopsis* and identified *cis1* (for ***C**O*$_2$ ***i**nsensitive **1***) that displayed significantly lower leaf surface temperature (0.68 ºC) relative to WT when challenged for 40 mins with 1,500 ppm [CO_2] (Fig. 1a,b). Genetic analysis revealed that this phenotype was caused by a single recessive Mendelian mutation (data not shown). To investigate the lesion in the *cis1* mutant further, we measured stomatal conductance (g_s). Fig. 1c and d show that in WT, challenge with 800 ppm CO_2 results in a reduction in g_s, whereas the response was attenuated in *cis1*. In contrast both *cis1* and WT displayed an increase in g_s when exposed to low (100 ppm) CO_2. We confirmed this response in *big-1*, a second independent allele of *cis1* (Supplemental Fig. S1). These data suggest that the *cis1* mutant is compromised in the stomatal response to elevated [CO_2].

Identification of the *CIS1* gene locus

We performed map-based gene cloning to identify the *CIS1* locus, and mapped the mutation to a 107kb region of chromosome III close to the *doc1* mutations (data not shown; Gil *et al.*, 2001). Seeds for T-DNA insertion lines of all annotated genes within this region were obtained from NASC and screened using infrared thermal imaging. A T-DNA insertion line (SALK_105495) of *At3g02260* was identified that displayed similar thermal behavior to the *cis1* mutant. Sequencing of *cis1* revealed a

single point mutation (G to A substitution) in locus *At3g02260* localized at a splicing acceptor site at position +8,542 (GT…AG to GT…AA) (Fig. 2a) which resulted in alternative spliced mRNAs as shown in Fig. S2. Real-time quantitative (Q) PCR, revealed that compared with WT, *cis1* (*At3g02260*) gene transcript abundance was reduced to a third (Fig. 2b).

At3g02260 has previously been named *BIG* and is annotated as encoding a large protein of 5098 amino acids, containing multiple conserved functional domains including three putative Zn-finger domains (Kanyuka *et al.*, 2003; Kasajima *et al.*, 2007). Our sequencing revealed that the original annotation is incorrect, as the open reading frame of *BIG* is 63bp shorter than predicted, because 30bp of the sequence of intron 1, 21 bp of intron 5 and 12bp of intron 7 had been annotated as part of the respective neighboring exons. Hence, the *BIG* ORF is 15,234bp long encoding a putative 5,077-amino-acid peptide as predicted by Gil and coworkers (Gil *et al.*, 2001).

Many alleles of *big* mutants *e.g. ga6, tir3, doc1, asr1, lpr1, elk1, asa1, umb1, crm1* and *rao3* have been independently isolated. All mutants are characterized by deficient organ elongation (dwarfism) and have altered root architecture, reduced apical dominance, defects in light responses, aberrant auxin transport. They also show altered sensitivities to GA, cytokinin, ethylene, low phosphate and water withholding treatments (Li *et al*., 1994; Ruegger *et al.*, 1997; Sponsel *et al.*, 1997; Gil *et al.*, 2001; Lease *et al.*, 2001; Kanyuka *et al.*, 2003; López-Bucio *et al.*, 2005; Kasajima *et al.*, 2007; Yamaguchi *et al.*, 2007; Ivanova *et al.*, 2014). Interestingly, insects and mammals possess homologs of the BIG protein and these are involved in signaling. Calossin/Pushover in *Drosophila melanogaster* and mammalian p600/UBR4 are homologs of BIG, both of which have CaM-binding domain and are likely involved in Ca^{2+} signaling (Xu *et al*., 1998; Parsons *et al*., 2015).

To confirm the identity of *cis1* we obtained two additional mutant alleles of *BIG*. *doc1-1* was originally isolated in a genetic screen for components of light signaling and harbours a single base change from G to A at position +5,514 (Fig. 2a) resulting in change from a conserved Cys residue change to Tyr. This missense *BIG* mutation perturbs auxin transport and plant growth (Gil *et al.*, 2001) but in our Q-PCR, analysis no change to the transcript abundance of *BIG* was detected (Fig. 2b). *big-1* harbours a T-DNA insertion in exon 9 before position +13,617 of the *BIG* gene (Kasajima *et al.*, 2007) (Fig. 2a). We detected no *BIG* transcript in this mutant by Q-PCR (Fig. 2b).

BIG is also involved in the control of stomatal development by elevated CO_2.

The data in Fig. 3a show that stomatal and epidermal pavement cell densities are greater in the *BIG* mutant alleles than WT ($P \leq 0.001$). This reflects the fact that both guard cells and epidermal cells were significantly smaller than WT (data not shown). Stomatal development is controlled by CO_2, with stomatal density and index typically reduced in plants grown under elevated [CO_2] (Woodward, 1987; Woodward & Kelly, 1995). We next investigated whether *BIG* has a role to play in the control of stomatal development by elevated [CO_2]. In WT growth at elevated [CO_2] resulted in a decrease in stomatal density and index (Fig. 3b,c). In marked contrast, under the same conditions, growth at elevated [CO_2] resulted in significant increases in both stomatal density and index in the *BIG* mutants (Fig. 3b,c). These data suggest that, in addition to controlling stomatal aperture, *BIG* is also required for the reduction in stomatal density and index caused by higher than ambient [CO_2].

The _BIG_ protein is involved in the signaling pathway by which elevated [CO_2] induces stomatal closure but not in the pathway through which elevated [CO_2] inhibits stomatal opening.

The results from the gas exchange experiments (Fig. 1c,d) prompted us to make direct measurements of stomatal responsiveness by quantifying changes in stomatal aperture

(Chater *et al.*, 2015). Fig. 4a shows that in contrast to WT the stomata of *cis1*, *big-1* and *doc1-1* mutants failed to close when subjected to 700 ppm CO_2. These data indicate that BIG is required for elevated CO_2-induced stomatal closure. Elevated [CO_2] is also known to inhibit light-induced stomatal opening (Mansfield *et al.*, 1990). In contrast to CO_2-induced stomatal closure, the inhibition of light-induced stomatal opening of the BIG mutants was similar to WT (Fig. 4b). The specific role of the *BIG* gene in the pathway by which elevated [CO_2] brings about stomatal closure is highlighted by our observation that the series of allelic mutants all display WT behavior in response to ABA. This holds for both ABA-induced stomatal closure and the inhibition by ABA of light-induced stomatal opening (Fig. 4c,d). The intact stomatal ABA response as well as the impaired CO_2 response were both observed in more than one of our laboratories underlining the robustness of the CO_2 specificity of the stomatal phenotype in *big* mutant alleles.

BIG is required for activation of S-type anion channels by elevated bicarbonates. S-type anion channels are recognized as one of the main players in guard cell signaling. They mediate the release of anions from guard cells and promote stomatal closure in response to diverse stimuli, including increased [CO_2] (Kollist *et al.*, 2011; Wang *et al.*, 2016). An increase in the cytoplasmic bicarbonate concentration activates S-type anion channels in guard cells and correlates with elevated [CO_2]-induced stomatal closure in diverse mutant backgrounds (Vahisalu *et al.*, 2008; Xue *et al.*, 2011; Merilo *et al.*, 2013). To understand the role of BIG in guard cell signaling further we investigated whether the activation of S-type anion channels by applied bicarbonate was impaired by mutations in *BIG*. In WT guard cell protoplasts, large anion currents were recorded when the pipette solution contained 11.5 mM free bicarbonate (Fig. 5b). However, in guard cell protoplasts of the *doc1-1* and *big-1* mutant alleles, currents were activated by the same concentration of bicarbonate in the pipette solution (Fig. 5e,h). At a voltage of -145 mV, the average activated currents

were -39.7 ± 4.6 pA for WT (Fig. 5c), -20.0 ± 2.0 pA for *doc1-1* mutant (Fig. 5f), -16.8 ± 1.8 for *big-1* mutant (Fig. 5i). The differences between WT and each mutant allele of *BIG* were statistically significant ($P \leq 0.01$). These results demonstrate that the BIG protein is required for elevated intracellular bicarbonate-induced activation of guard-cell plasma-membrane S-type anion channel currents that function in CO_2-induced stomatal closure and further reinforce the importance of BIG in stomatal closure.

Discussion

BIG is involved in stomatal closure induced by elevated CO_2 but not in elevated CO_2-induced inhibition of stomatal opening.

We conducted a genetic screen that resulted in the identification of a novel allele of the *BIG* gene that we call *CIS1* that plays a regulatory role in stomatal function and development. Our phenotypic analyses revealed that *CIS1* is involved in the reduction in stomatal conductance induced by elevated CO_2 (Fig. 1b,c; Fig. S1). On the surface of a leaf, during the day, stomata are exposed to frequently conflicting signals from the environment. Guard cells integrate these signals and the overall result is the optimization of gas exchange under the prevailing environmental conditions. Looking at this more closely, in the case of stomatal closure it is necessary to stimulate the processes associated with the loss of guard cell turgor while simultaneously inhibiting the cellular reactions involved in solute accumulation and stomatal opening. The opening and closure responses are physiologically distinct and are not the reverse of each other (Assmann, 1993; Li *et al.*, 2000). When we investigated the role of *BIG* in these processes we found, intriguingly, that it was only involved in elevated CO_2-induced stomatal closure. In marked contrast all of the BIG mutants exhibited WT behavior in our CO_2-inhibition of light-stimulated stomatal opening bioassay (Fig. 4a,b). To extend our investigation of the role of BIG in the regulation of stomatal aperture we also investigated whether it played a role in stomatal closure induced by

289 ABA. The data in Fig. 4 (c,d) clearly indicate that BIG is neither involved in ABA-
290 promoted closure nor in ABA-inhibited light-induced opening. Because *BIG* encodes
291 a protein that, in guard cells, is only involved in CO_2-induced closure and not CO_2-
292 inhibited opening, this makes it possible at the molecular level to distinguish, and to
293 start to define these different processes. In this sense these data fit well with the
294 observation that in molecular terms ABA-induced stomatal closure is distinct from the
295 inhibition of opening by ABA. Examples include GPA1, which is involved in ABA-
296 inhibition of opening but not in closure (Wang *et al.*, 2001), a sphingosine-1-
297 phosphate phosphatase, long-chain base phosphate lyase double mutant (*sppasedpl1*)
298 that displays WT behavior during ABA-induced closure but is slightly impaired in the
299 ABA inhibition of stomatal opening response (Worrall *et al.*, 2008), PI-phospholipase
300 C which is involved in the ABA-inhibition of opening but not closure (Mills *et al.*,
301 2004) and the observation that some members of PYR/PYL ABA receptor family
302 involved in stomatal opening inhibition are different from those involved in stomatal
303 closure induction (Yin *et al.*, 2013). The second striking result to emerge from these
304 experiments is that BIG is not involved in ABA-induced reductions in stomatal
305 aperture (Fig. 4c,d). This suggests that the BIG protein lies upstream of the point of
306 convergence of the guard cell CO_2 and ABA signaling pathways (Webb &
307 Hetherington, 1997; Xue *et al.*, 2011; Merilo *et al.*, 2013; Chater *et al.*, 2015;
308 Jakobson *et al.*, 2016; Yamamoto *et al.*, 2016). Looking downstream of the point of
309 convergence it is well known that both ABA- and CO_2-induced stomatal closure
310 involve activation of slow anion channels (Kim *et al.*, 2010; Assmann & Jergla, 2016;
311 Engineer *et al.*, 2016). Our data reveal that mutations in BIG depressed the activation
312 of S-type anion channels by bicarbonate (Fig. 5) in line with the impaired elevated
313 [CO_2]-induced stomatal closure. A recent study by Yamamoto and coworkers
314 provided evidence that different parts of SLAC1 are separately responsible for sensing
315 ABA and CO_2 signals (Yamamoto *et al.*, 2016). It is the transmembrane domain of
316 SLAC1 channels that perceives CO_2 signals in contrast to the N- and C terminal ends

of SLAC1 which are responsible for ABA signaling in *Arabidopsis* (Brandt *et al.*, 2015; Yamamoto *et al.*, 2016). Further investigation is needed to determine whether the activation of S-type anion channels by ABA is affected by the loss of *BIG* gene function.

BIG is also involved in the control of stomatal development by elevated CO_2.

Fig. 3a shows that mutations in BIG result in significant increases in guard and epidermal pavement cell densities consistent with the findings of Guo *et al*. (2013). Growth at elevated [CO_2] typically results in a reduction in stomatal index and density (Hetherington & Woodward, 2003; Assmann & Jergla, 2016; Engineer *et al.*, 2016). The results in Fig. 3b and c clearly show that, in marked contrast to WT, stomatal indices and density of BIG mutants increased when the plants were grown at 1,000 ppm CO_2. It is likely, as with *ßca1ca4, epf2* and *hic* mutants (Gray *et al*., 2000; Engineer *et al*., 2014), that loss of BIG function relieves the elevated [CO_2]-mediated repression of stomatal development. How might BIG bring about an effect on CO_2-mediated stomatal development? One possibility that would merit future investigation is that this is an auxin-related response. The *BIG* gene has been reported to encode a protein associated with auxin transport (Gil *et al.*, 2001; Kanyuka *et al.*, 2003) and is specifically required in the process by which auxin inhibits endocytosis and promotes its own efflux from cells (Paciorek *et al.*, 2005). In this context it is worth noting that evidence is emerging that auxin inhibits stomatal development. Mutants disrupted in the TAA1/TAR auxin biosynthesis pathway or polar auxin transport and strong perturbations in auxin signaling, as observed in multiple *tir1/afb* auxin receptor mutants, cause stomatal clustering (Balcerowicz *et al.*, 2014; Le *et al.*, 2014; Zhang *et al.*, 2014). However, we observed no stomatal clustering in the *cis1* and related mutants. Further work will be required to reveal whether disruptions to auxin signaling underlie the BIG stomatal mutant phenotype.

In conclusion, we demonstrate that, in *Arabidopsis,* the BIG protein is involved in both the elevated [CO_2]-mediated control of stomatal closure and density. Our results reveal we have identified a component that is involved in the signaling pathway by which elevated CO_2 promotes stomatal closure. However, BIG is neither involved in the elevated [CO_2]-mediated inhibition of light induced opening nor stomatal closure initiated by ABA. These data indicate that elevated [CO_2]-mediated closure and inhibition of opening are, in molecular terms, distinguishable. Our data suggest that BIG lies upstream of the point of convergence of ABA and CO_2 or resides in an, as yet undefined parallel signaling pathway that converges at or above the SLAC1 ion channel.

Materials and Methods

Plant Growth

All *Arabidopsis thaliana* lines used were in the Columbia background (Col-0). Seeds of *doc1-1* and *big-1* were obtained from NASC (the European Arabidopsis Stock Centre, http://arabidopsis.org.uk). Seed germination and plant growth were as described previously (Liang *et al.*, 2010).

Mutant screen

To identify genes required for stomatal CO_2 responses we screened 20,000 seeds from an Arabidopsis EMS M2 population representing 40 independent pools (each pool corresponding to approximately 1,000 M1 plants) by infrared thermal imaging (Wang *et al.*, 2004; Xie *et al.*, 2006). Screening was carried out on 3-4 weeks old plants in a purpose-built chamber (84 x 68 x 20 cm), located inside a controlled environment room. CO_2 concentration inside the chamber was controlled externally from CO_2 cylinders. Air flow in the chamber was maintained at 0.03 m sec^{-1} using fans. Relative humidity inside the chamber was about 60%, temperature was 22°C and light intensity 120 µmol m^{-2} s^{-1}. Plants were placed in the chamber and exposed to 360

ppm [CO_2] cylinder (balanced air mixture). After 40 mins thermal images were captured and the plants then exposed to 1,500 ppm [CO_2] (1,500 ppm [CO_2] cylinder (balanced air mixture) for a further 40 minutes and thermal images captured. Pairs of images were compared to identify putative CO_2 response mutants. Infrared thermal imaging was performed using an Inframetrics middle infrared (3.4-5 μm) camera model SC1000E (FLIR Systems). Images were stored in a ThermaCam Image file format (IMG) and analysed with the ThermaCam™ Researcher 2001 software (FLIR Systems, 2001 Inc., USA). Mutants exhibiting altered leaf thermal profiles compared to WT were selected, self-pollinated and seeds (M3) were collected for further investigation. Backcross seeds (F1s) were obtained by using mutant lines as female and Col-0 as male. The F2 was used for segregation analysis. Mutants segregating in the F2 were backcrossed to WT Col-0 for another two generations before being used for fine mapping and phenotyping.

Map based mutant gene cloning

cis1 mutants were outcrossed to WT plants in the Landberg *erecta* background (L*er*) and the segregating F2 seedlings were screened using infrared thermography. A total of 868 *cis1* mutants were used for mapping. 22 SSLP markers were used for bulked segregant analysis as described (Lukowitz *et al.*, 2000). The *Arabidopsis* SNP collections (http://www.arabidopsis.org/) were used for designing SSLP, CAPS and dCAPS markers for the fine mapping. The mutation was narrowed down into an approximate 100kb region at the top arm of Chromosome III between SSLP marker nga172 and CAPS marker CA1 and is adjacent to SSLP marker nga32. T-DNA insertion lines representing all the annotated genes within this region were obtained from NASC and screened using infrared thermal imaging. A T-DNA insertion line (SALK_105495) of *At3g02260* which also showed morphologically similarity to the mutant '*cis1*' was identified. We performed an allelism tests using the F1 progeny of the *cis1* and *big-1* (SALK_105495) cross using thermal imaging. This confirmed that

401 *cis1* and *big-1* are allelic to each other. We used PCR based genotyping and gene
402 sequencing to confirm the presence of a T-DNA insertion in gene A*t3g02260* of the
403 SALK_105495 line and a single point mutation in gene *At3g02260* of the *cis1* mutant.
404
405 **Measurements of stomatal density, index, aperture and cell viability**
406 Stomatal density and index were measured on leaf abaxial surfaces as described
407 (Chater *et al.*, 2015). The effect of CO_2 on stomatal aperture was measured using the
408 isolated epidermal strip bioassay technique as previously described (Chater *et al.*,
409 2015). Forty stomatal pores were measured per treatment in three separate replicated
410 tests. To avoid experimenter bias, all the aperture measurements were performed blind.
411 Cell viability was assessed as described in Chater *et al*. (2015). Experiments on
412 independently grown plant material were carried out three times and data analysed by
413 SigmaPlot 10.
414
415 **Gas exchange measurements**
416 Time-resolved stomatal conductance analyses of intact leaves of five week-old plants
417 were conducted using a Li-6400 gas exchange analyzer with a fluorometer chamber
418 (Li-Cor Inc.) as described by Hu *et al.* (2010). The photon flux density was set at 150
419 μmol m^{-2} s^{-1}, temperature and relative humidity were held at 21°C and approximately
420 60-70%, respectively. Stomatal conductance was stabilized at 400 ppm CO_2 (as
421 ambient concentration) for 30 min and then shifted to 800 ppm for another 30 min
422 before shifted to 100 ppm for 1.5h. Data shown are means ± SE, n=4 leaves for each
423 genotype.
424
425 **Patch clamp experiments**
426 *Arabidopsis* guard cell protoplasts were isolated according to the procedure described
427 previously (Siegel *et al*., 2009). The whole-cell currents were recorded using a patch
428 clamp amplifier (Axopatch 200B) and a digitizer (Digidata 1550). CO_2/bicarbonate -

activated S-type anion currents were recorded as described before (Xue *et al.*, 2011). The bath solution contained 30 mM CsCl, 2 mM $MgCl_2$, 1mM $CaCl_2$ and 10 mM Mes/Tris pH 5.6. The pipette solution contained 150 mM CsCl, 2 mM $MgCl_2$, 6.7 mM EGTA, 6.03 mM $CaCl_2$ (2 μM free Ca^{2+}), 5 mM Mg-ATP, 10 mM HEPES/Tris pH7.1. Bicarbonate was freshly added to the pipette solution before patching the protoplasts each day. At pH 7.1, 11.5 mM free bicarbonate was balanced with 2 mM free CO_2 in the pipette solution. For more details please consult with Xue *et al.* (2011).

RT-PCR and quantitative RT-PCR analysis

Total RNA from aerial parts of the plants was prepared using RNeasy total RNA mini kit (Qiagen) and digested with RNase-free DNase I (Thermo scientific), and the absence of genomic DNA contamination was confirmed by PCR using RNA as template without reverse transcription. First strand cDNA was synthesized using Superscript II® reverse transcriptase (Invitrogen) and oligo $d(T)_{15-18}$ (Promega) mRNA primer with 1 μg of total RNA as the template. cDNA corresponding to 20 ng of total RNA and 300 nM of each primer were used in PCR reactions. The primers for RT-PCR amplification *BIG* fragments were: primer pair1, F1 (5'-CAGCAAGCTCTATACCTTCAG-3') and R1, (5'- TCCATCCATCCACTCAACTC -3'); primer pair 2, F2 (5'-GTCTTCTACTTCACTGACCAACTCC-3') and R2, (5'-TCCATCTTCTTCTTCCTCTACATCC -3'); Actin7 was amplified with forward primer (5'-TGTTCCCAAGTATTGTTGGTCGTC-3') and reverse primer (5'-TGCTGAGGGATGCAAGGATTGATC-3') as a loading control. The PCR conditions were as follows: 1 cycle (94°C, 5 min), 35 cycles (94°C, 30 s; 62°C, 30 s; 72°C, 1min), 1 cycle (72°C, 7 min). Q-PCR was carried out on a Mx3005P (Stratagene) or an ECO (Illumina) real-time PCR thermal cycler in a total reaction volume of 20μL using the SYBR green dye PCR Master Mix (Thermo scientific), using these conditions, 95°C for 10 min, 40 two-step cycles at 95°C for 15 sec and 60°C for 1 min, followed by dissociation melting curve analysis to determine the PCR

specificity. The gene-specific primers used for *BIG* are F: 5'-GAATGGGAAGGAGCTATGTTG-3' and R: 5'-GATACTGTGCTAAGGGAACTG-3'; for *Actin3* (*At3g53750)* are F: 5'-GGCAGAATATGATGAGTCAGG-3' and R: 5'-AAAGAAGAGCAGAGAACGAAG-3'. The relative RNA levels were calculated from cycle threshold (C_T) values according to the ΔC_T method, and relative target mRNA levels were normalized to *Actin3* mRNA levels. Reactions were repeated independently three times with similar results.

Acknowledgements

The authors are grateful to Prof. HMO Leyser (University of Cambridge, UK) for the gift of the EMS-mutagenised Arabidopsis population. Y.-K.L. acknowledges National Key Research and Development Program (2016YFD0100600) and National Natural Science Foundation of China (31171356, 31470360) for providing research funding. A.M.H. and J.E.G. acknowledge the support of the UK Biotechnological and Biological Sciences Research Council. Research in J.I.S. laboratory was supported by National Science Foundation (MCB-16162360 and NIH (GM060396) grants. Research in J.K. laboratory was supported by grants from the Deutsche Forschungsgemeinschaft (DFG). S.X. was supported by NSFC (31670267) and the Fundamental Research Funds for the Central Universities (2662015PY213, 2014PY065). H.H. received support by the 1000-talents Plan for young researchers from China and the Fundamental Research Funds for the Central Universities (2662017PY034).

Author contributions

A.M.H. conceived the study. Y.-K.L. and A.M.H. designed the research. Y.-K.L., J.H., R.-X.Z., K.P., C.T., S.L., S.X., A.L., H.H., J.Z., K.E.H. and K. H. conducted the experiments. J.H., J.K., M.R.M., J.E.G., J.I.S., Y.-K.L. and

A.M.H. analyzed data. A.M.H., Y.-K.L. and J.E.G. wrote the manuscript. All authors read and approved the manuscript.

Reference

Assmann SM. 1993. Signal transduction in guard cells. *Annual review of cell biology* **9**: 345–375.

Assmann SM, JeglaT. 2016. Guard cell sensory systems: recent insights on stomatal responses to light, abscisic acid, and CO_2. *Current Opinion in Plant Biology* **33**: 157–167.

Balcerowicz M, Ranjan A, Rupprecht L, Fiene G, Hoecker U. 2014. Auxin represses stomatal development in dark-grown seedlings via Aux/IAA proteins. *Development* **141**: 3165–3176.

Brandt B, Munemasa S, Wang C, Nguyen D, Yong T, Yang PG, Poretsky E, Belknap TF, Waadt R, Aleman F, Schroeder JI. 2015. Calcium specificity signaling mechanisms in abscisic acid signal transduction in Arabidopsis guard cells. *Elife* **4**: 03599.

Chater C, Peng K, Movahedi M, Dunn JA, Walker HJ, Liang Y-K, McLachlan DH, Casson S, Isner JC, Wilson I *et al.* 2015. Elevated CO_2-induced responses in stomata require ABA and ABA signaling. *Current Biology* **25**: 2709–2716.

Darwin F. 1904. On a self-recording method applied to the movements of stomata. *Botanical Gazette* **37**: 81–105.

Engineer CB, Ghassemian M, Anderson JC, Peck SC, Hu H, Schroeder JI. 2014. Carbonic anhydrases, EPF2 and a novel protease mediate CO_2 control of stomatal development. *Nature* **513**: 246–250.

Engineer CB, Hashimoto-Sugimoto M, Negi J, Israelsson-Nordström M, Azoulay-Shemer T, Rappel WJ,Iba K, Schroeder JI. 2016. CO_2 sensing and CO_2 regulation of stomatal conductance: advances and open questions. *Trends in Plant Science* **21**: 16–30.

Franks PJ, Leitch IL, Ruszala EM, Hetherington AM, Beerling DJ.2012. Physiological framework for adaptation of stomata to CO_2 from glacial to future concentrations. *Philosophical Transactions of the Royal Society B: Biological Sciences* **367**: 537–546.

Gil P, Dewey E, Friml J, Zhao Y, Snowden KC, Putterill J, Palme K, Estelle M, Chory J. 2001. BIG: a calossin-like protein required for polar auxin transport in *Arabidopsis*. *Genes Development* **15**: 1985–1997.

Gray JE, Holroyd GH, Van Der Lee FM, Baharmi AR, Sijmons PC, Woodward FI, Schuch W, Hetherington AM. 2000. The HIC signalling pathway links CO_2 perception to stomatal development. *Nature* **408**: 713–716.

Hashimoto M, Negi J, Young J, Israelsson M, Schroeder JI, Iba K. 2006. *Arabidopsis* HT1 kinase controls stomatal movements in response to CO_2. *Nature Cell Biology* **8**: 391–397.

Hashimoto-Sugimoto M, Negi J, Monda K, Higaki T, Isogai Y, Nakano T, Hasezawa S, Iba K. 2016. Dominant and recessive mutations in the Raf-like kinase HT1 gene completely disrupt stomatal responses to CO_2 in *Arabidopsis*. *Journal of Experimental Botany* **67**: 3251–3261.

Hetherington AM, Woodward FI. 2003. The role of stomata in sensing and driving environmental change. *Nature* **424**: 901–908.

Hõrak H, Sierla M, Tõldsepp K, Wang C, Wang Y-S, Nuhkat M, Valk E, Pechter P, MeriloE,Salojärvi J *et al.* 2016. A dominant mutation in the HT1 kinase uncovers roles of MAP kinases and GHR1 in CO_2-induced stomatal closure. *Plant Cell* **28**: 2493–2509.

Hu HH, Boisson-Dernier A, Israelsson-Nordstrom M, Böhmer M, Xue S, Ries A, Godoski J, Kuhn JM, Schroeder JI. 2010. Carbonic anhydrases are upstream regulators of CO_2-controlled stomatal movements in guard cells. *Nature Cell Biology* **12**: 87–93.

Ivanova A, Law SR, Narsai R, Duncan O, Lee JH, Zhang B, Van Aken O, Radomiljac JD, Van Der Merwe M, Yi K *et al.* 2014. A functional antagonistic relationship between auxin and mitochondrial retrograde signaling regulates ALTERNATIVE OXIDASE1a expression in *Arabidopsis thaliana. Plant Physiology* **165**: 1233–1254.

Jakobson L, Vaahtera L, Tõldsepp K, Nuhkat M, Wang C, Wan YS,Tang J, Xiao CL, Xu Y, Talas UG *et al.* 2016. Natural Variation in *Arabidopsis* Cvi-0 Accession Reveals an Important Role of MPK12 in Guard Cell CO_2 Signaling. *PLoS Biology* **14**: e2000322.

Kanyuka K, Praekelt U, Franklin KA, Billingham OE, Hooley R, Whitelam GC, Halliday KJ. 2003. Mutations in the huge *Arabidopsis* gene BIG affect a range of hormone and light responses. *Plant Journal* **35**: 57–70.

Kasajima I, Ohkama-Ohtsun, Ide Y, Hayashi H, Yoneyama T, Suzuki Y, Naito S, Fujiwara T. 2007. The *BIG* gene is involved in regulation of sulfur deficiency-responsive genes in *Arabidopsis thaliana*. *Physiologia Plantarum* **129**: 351–363.

Kim TH, Böhmer M, Hu HH, Nishimura N, Schroeder JI. 2010. Guard cell signal transduction network: advances in understanding abscisic acid, CO_2, and Ca^{2+} signaling. *Annual Review of Plant Biology* **61**: 561–591.

Kollist H, Jossier M, Laanemets K, Thomine S. 2011. Anion channels in plant cells. *FEBS Journal* **278**: 4277–4292.

Le J, Liu XG, Yang KZ, Chen XL, Zou JJ, Wang HZ, Ding ZJ *et al.* 2014. Auxin transport and activity regulate stomatal patterning and development. *Nature Communications* **5**: 3090.

Lease KA, Wen JQ, Li J, Doke JT, Liscum E, Walker JC. 2001. A mutant *Arabidopsis* heterotrimeric G-protein β subunit affects leaf, flower, and fruit development. *Plant Cell* **13**: 2631–2641.

Li H-M, Altschmied L, Chory J. 1994. *Arabidopsis* mutants define downstream branches in the phototransduction pathway. *Genes Development* **8**: 339–349.

Li J, Wang XQ, Watson MB, Assmann SM. 2000. Regulation of abscisic acid-induced stomatal closure and anion channels by guard cell AAPK kinase. *Science* **287**: 300–303.

Liang Y-K, Xie XD, Lindsay SE, Wang YB, Masle J, Williamson L, Leyser O, Hetherington AM. 2010. Cell wall composition contributes to the control of transpitration efficiency in *Arabidopsis thaliana*. *Plant Journal* **64**: 679–686.

López-Bucio J, Hernández-Abreu E, Sánchez-Calderón L, Pérez-Torres A, Rampey RA, Bartel B, Herrera-Estrella L. 2005. An auxin transport independent pathway is involved in phosphate stress-induced root architectural alterations in *Arabidopsis*. Identification of BIG as a mediator of auxin in pericycle cell activation. *Plant Physiology* **137**: 681–691.

Lukowitz W, Gillmor CS, Scheibel W-R. 2000. Positional cloning in *Arabidopsis*. Why it feels good to have a genome initiative working for you. *Plant Physiology* **123**: 795–806.

Mansfield TA, Hetherington AM, Atkinson CJ. 1990. Some Current Aspects of Stomatal Physiology. *Annual Review of Plant Physiology and Plant Molecular Biology* **41**: 55–75.

Merlot S, Mustilli AC, Gently B, North H, Lefebvre V, Sotta B, Vavasseur A, Giraudat J. 2002. Use of infrared thermal imaging to isolate *Arabidopsis* mutants defective in stomatal regulation. *Plant Journal* **30**: 601–609.

MeriloE,Laanemets K, Hu HH, Xue S, Jakobson L, Tulva I, Gonzalez-Guzman M, Rodriguez PL, Schroeder JI, Broschè M *et al.* 2013. PYR/RCAR receptors contribute to ozone-, reduced air humidity-, darkness-, and CO_2-induced stomatal regulation. *Plant Physiology* **162**: 1652–1668.

Mills LN, Hunt L, Leckie CP, Aitken FL, Wentworth M, McAinsh MR, Gray JE, Hetherington AM. 2004. The effects of manipulating phospholipase C on guard cell ABA-signalling. *Journal of Experimental Botany* **55**: 199–204.

Negi J, Matsuda O, Nagasawa T, Oba Y, Takahashi H, Kawai-Yamada M, Uchimiya H, Hashimoto M, Iba K. 2008. CO_2 regulator SLAC1 and its homologues are essential for anion homeostasis in plant cells. *Nature* **452**: 483–486.

Paciorek T, Zazimalova E, Ruthardt N, Petráš ek J, Stierhof Y-D, Kleine-Vehn J, Morris DA, Emans N, Jürgens G, Geldner N *et al.* 2005. Auxin inhibits endocytosis and promotes its own efflux from cells. *Nature* **435**: 1251–1256.

Raskin I, Ladyman JA. 1988. Isolation and characterization of a barley mutant with abscisic-acid-insensitive stomata. *Planta* **173**: 73–78.

Ruegger M, Dewey E, Hobbie L, Brown D, Bernasconi P, Turner J, Muday G, Estelle M. 1997. Reduced naphthylphthalamic acid binding in the *tir3* mutant of *Arabidopsis* is associated with a reduction in polar auxin transport and diverse morphological defects. *Plant Cell* **9**: 745–757.

Siegel RS, Xue S, Murata Y, Yang Y, Nishimura N, Wang A, Schroeder JI. 2009. Calcium elevation-dependent and attenuated resting calcium-dependent abscisic acid induction of stomatal closure and abscisic acid-induced enhancement of calcium sensitivities of S-type anion and inward-rectifying K^+ channels in *Arabidopsis* guard cells. *Plant Journal* **59**: 207–220.

Sponsel VM, Schmidt FW, Porter SG, Nakayama M, Kohlstruk S, Estelle M. 1997. Characterization of new gibberellin-responsive semidwarf mutants of *Arabidopsis*. *Plant Physiology* **115**: 1009–1020.

Tian W, Hou C, Ren Z, Pan Y, Jia J, Zhang H, Bai F, Zhang P, Zhu H, He Y *et al.* 2015. A molecular pathway for CO_2 response in *Arabidopsis* guard cells. *Nature Communications* **6**: 6057.

Vahisalu T, Kollist H, Wang YF, Nishimura N, Chan WY, Valerio G, Lamminmäki A, Brosché M, Moldau H, Desikan R *et al.* 2008. SLAC1 is required for plant guard cell S-type anion channel function in stomatal signalling. *Nature* **452**: 487–491.

Vavasseur A, Raghavendra AS. 2005. Guard cell metabolism and CO_2 sensing. *New Physiologist* **165**: 665–682.

Wang C, Hu H, Qin X, Zeise B, Xu D, Rappel WJ, Boron WF, Schroeder JI. 2016. Reconstitution of CO_2 regulation of SLAC1 anion channel and function of CO_2-permeable PIP2; 1 aquaporin as CARBONIC ANHYDRASE4 interactor. *Plant Cell* **28**: 568–582.

Wang XQ, Ullah H, Jones AM, Assmann SM. 2001. G protein regulation of ion channels and abscisic acid signaling in *Arabidopsis* guard cells. *Science* **292**: 2070–2072.

Wang YB, Holroyd G, Hetherington AM, Ng CKY. 2004. Seeing 'cool' and 'hot'-infrared thermography as a tool for non-invasive, high-throughput screening of *Arabidopsis* guard cell signalling mutants. *Journal of Experimental Botany* **55**: 1187–1193.

Webb AAR, Hetherington AM. 1997. Convergence of the abscisic acid, CO_2, and extracellular calcium signal transduction pathways in stomatal guard cells. *Plant Physiology* **114**: 1557–1560.

Woodward FI. 1987. Stomatal numbers are sensitive to increases in CO_2 from pre-industrial levels. *Nature* **327**: 617–618.

Woodward FI, Kelly CK. 1995. The influence of CO_2 concentration on stomatal density. *New Phytologist* **131**: 311–327.

Worrall D, Liang Y-K, Alvarez S, Holroyd GH, Spiegel S, Panagopulos M, Gray JE, Hetherington AM. 2008. Involvement of sphingosine kinase in plant cell signalling. *Plant Journal* **56**: 64–72.

Xie XD, Wang YB, William L, Holroyd GH, Tagliavia C, Murchie E, Theobald J, Knight MR, Davies WJ, Leyser HM *et al.* 2006. The identification of genes involved in stomatal response to reduced atmospheric relative humidity. *Current Biology* **16**: 882–887.

Xue S, Hu H, Ries A, Merilo E, Kollist H, Schroeder JI. 2011. Central function of bicarbonate in S-type anion channel activation and OST1 protein kinase in CO_2 signal transduction in guard cell. *EMBO Journal* **30**: 1645–1658.

Yamaguchi N, Suzuki M, Fukaki H, Morita-Terao M, Tasaka M, Komeda Y. 2007. CRM1/BIG-mediated auxin action regulates *Arabidopsis* inflorescence development. *Plant Cell Physiology* **48**: 1275–1290.

Yamamoto Y, Negi J, Wang C, Isogai Y, Schroeder JI, Iba K. 2016. The transmembrane region of guard cell SLAC1 channels perceives CO_2 signals via an ABA-independent pathway in *Arabidopsis*. *Plant Cell* **28**: 557–567.

Yin Y, Adachi Y, Ye W, Hayashi M, Nakamura Y, Kinoshita T, Mori IC, Murata Y. 2013. Difference in abscisic acid perception mechanisms between closure induction and opening inhibition of stomata. *Plant Physiology* **163**: 600–610.

Zhang JY, He SB, Li L, Yang HQ. 2014. Auxin inhibits stomatal development through MONOPTEROS repression of a mobile peptide gene STOMAGEN in mesophyll. *Proceedings of the National Academy of Sciences of the United States of America* **111**: E3015–E3023.

Figure Legends:

Fig. 1. The *cis1* mutant displays a lower leaf surface temperature under elevated CO_2 than WT.

(a) Infrared thermograms showing that the leaf surface temperature of the *cis1* mutant is lower than that of WT when the plants are exposed to 1,500 ppm CO_2.

(b) The average leaf surface temperature of the *cis1* mutant is approximate 0.68ºC lower than that of WT plant when both are exposed to 1,500 ppm CO_2. Bars=mean ±SE (Student's *t* test, **P ≤0.001, n=20).

(c) In contrast to WT, the *cis1* mutant fails to display elevated (800 ppm) CO_2-induced reduction in stomatal conductance, but exhibits a WT response when exposed to low (100 ppm) CO_2 (representative data, n=4).

(d) Relative stomatal conductance in (c) (presented is representative data, n=4).

Fig. 2. *cis1* is a new allele of the *BIG* gene.

(a) Schematic structure of the *BIG* gene. The intron and exon organization of the *BIG* gene shown was determined by comparison of the cDNAs obtained by RT-PCR and genomic sequences from the *Arabidopsis* WT Col-0. Closed boxes indicate exons, and lines between boxes indicate introns. The locations of the single base mutations and T-DNA insertion of *cis1*, *doc1-1* and *big-1* are indicated. Diagram not to scale.

(b) The relative mRNA levels of *BIG* mutant alleles quantified by Q-PCR with a pair primers (F and R) with binding sites shown on (a). Values are mean ± SE, n=3.

Fig. 3. *BIG* gene mutants have higher stomatal density than WT.

(a) Compared with WT, *BIG* mutants exhibit increased stomata and epidermal pavement cells (labelled as "Epidermis") density when grown at ambient [CO_2]. Error bars represent ± SE (Mann-Whitney rank sum test, **P ≤ 0.001, n=72).

(b) Stomatal density of WT and *BIG* mutant seedlings grown at ambient 450 ppm and elevated 1,000 ppm [CO_2]. When grown at 1,000ppm [CO_2] mean stomatal density of

WT was significantly reduced compared with growth at ambient [CO_2] (Mann-Whitney rank sum test, ** $p \leq 0.001$, $n > 20$), whereas in the *BIG* gene alleles stomatal density increased in these conditions (Student's *t* test, ** $p \leq 0.001$, $n > 20$).

(c) Stomatal index of WT and *BIG* mutant seedlings grown at 450 ppm and 1,000 ppm [CO_2]. When grown at 1,000 ppm mean stomatal index of WT was significantly reduced compared with growth at ambient [CO_2] (Student's *t* test, **$p \leq 0.001$, $n > 20$), whereas in the *BIG* gene mutants' stomatal index increased in these conditions (Student's *t* test, or Mann-Whitney rank sum test, **$p \leq 0.001$, $n > 20$).

Fig. 4. Stomatal responses of *BIG* gene mutants to elevated CO_2 or exogenous ABA.

(a) Elevated CO_2-induced stomatal closure is impaired in *BIG* gene mutants. Values are mean ±SE (Mann-Whitney rank sum test, **$P \leq 0.001$, $n=40$).

(b) Elevated CO_2 induced inhibition of stomatal opening is not compromised in *BIG* gene mutants. Error bars represent SE ($n=40$).

(c) ABA-induced stomatal closure is not compromised in *BIG* gene mutants. Bars=mean ±SE ($n=40$).

(d) The inhibition of light-induced stomatal opening by ABA is not compromised in *BIG* gene mutants. Values are mean ± SE ($n=40$).

Fig. 5. Bicarbonate-activated S-type anion currents were suppressed in *BIG* mutant guard cell protoplasts.

(a) Typical recording in wild type guard cell protoplasts without bicarbonate.

(b) Typical recording of 11.5 mM $[HCO_3^-]_i$- activated S-type anion currents in wild type guard cell protoplasts.

(c) Average current-voltage relationships of whole-cell currents as recording in (a) (open circles, $n=5$) and (b) (filled circles, $n=7$).

(d) Representative recording in *doc1-1* mutant guard cell protoplasts without bicarbonate added in the pipette solution.
(e) Representative whole-cell current recording in *doc1-1* mutant guard cell protoplasts with 11.5 mM $[HCO_3^-]_i$ added in the pipette solution.
(f) Average current-voltage relationships of whole-cell currents as recording in (d) (open circles, n=5) and (e) (filled circles, n=8).
(g) Representative recording in *big-1* mutant guard cell protoplasts without bicarbonate added in the pipette solution.
(h) Representative whole-cell current recording in *big-1* mutant guard cell protoplasts with 11.5 mM $[HCO_3^-]_i$ bicarbonate added in the pipette solution.
(i) Average current-voltage relationships of whole-cell currents as recording in (g) (open circle, n=6) and (h) (filled circles, n=8).

Fig. S1. (a) In contrast to WT, the *big1* mutant fails to display elevated (800 ppm) CO_2-induced reduction in stomatal conductance, but exhibits a WT response when exposed to low (100 ppm) CO_2 (representative data, n=4). (b) Relative stomatal conductance in (a) (representative data, n=4).

Fig. S2. PCR amplification of the *BIG* fragment from cDNAs of WT and mutant plants showed a complex PCR band pattern of *cis1* and only truncated *BIG* transcript present in *big-1* whereas no change in mRNA abundance is detected in the *doc1-1* mutant. Primer binding sites as indicated in Fig. 2a. *ACTIN* was used as a reference gene.

Fig. S3. Epidermal cell density of WT and *BIG* gene mutant seedlings grown at elevated 1,000 ppm $[CO_2]$.

Supplementary Information. Determination of the intron-exon structure of *BIG* by DNA sequencing.

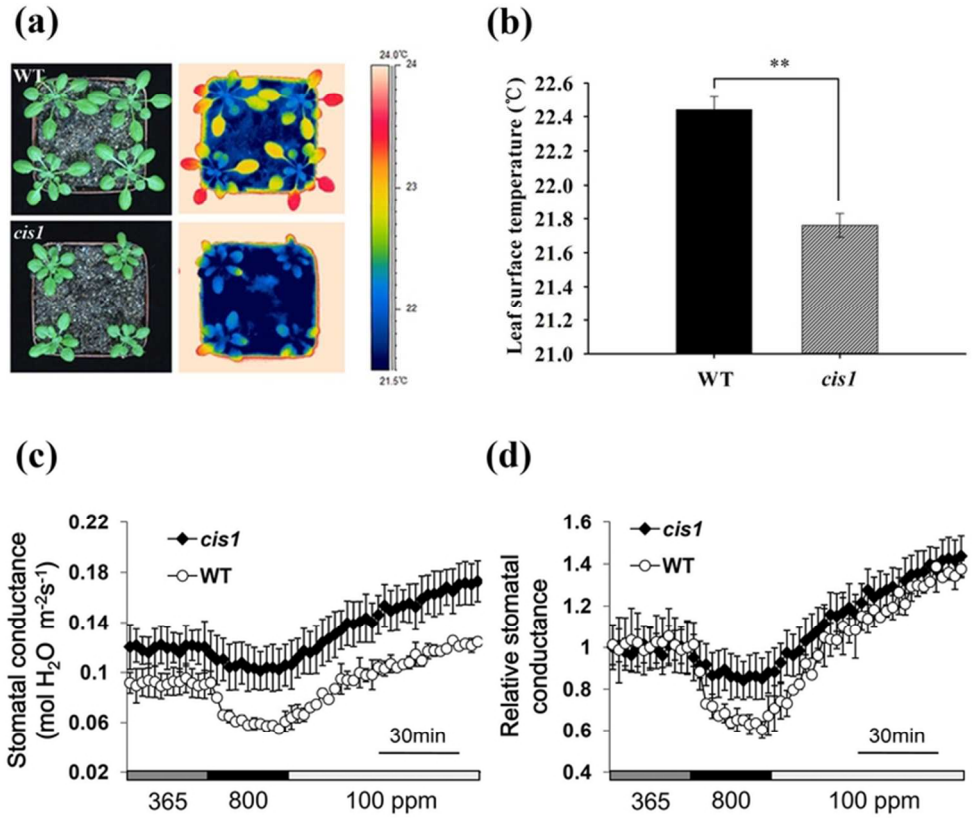

Fig. 1. The cis1 mutant displays a lower leaf surface temperature under elevated CO2 than WT. (a) Infrared thermograms showing that the leaf surface temperature of the cis1 mutant is lower than that of WT when the plants are exposed to 1,500 ppm CO2. (b)The average leaf surface temperature of the cis1 mutant is approximate 0.68ºC lower than that of WT plant when both are exposed to 1,500 ppm CO2. Bars=mean ±SE (Student's t test, **P ≤0.001, n=20). (c) In contrast to WT, the cis1 mutant fails to display elevated (800 ppm) CO2-induced reduction in stomatal conductance, but exhibits a WT response when exposed to low (100 ppm) CO2 (representative data, n=4). (d) Relative stomatal conductance in (c)(presented is representative data, n=4).

67x57mm (300 x 300 DPI)

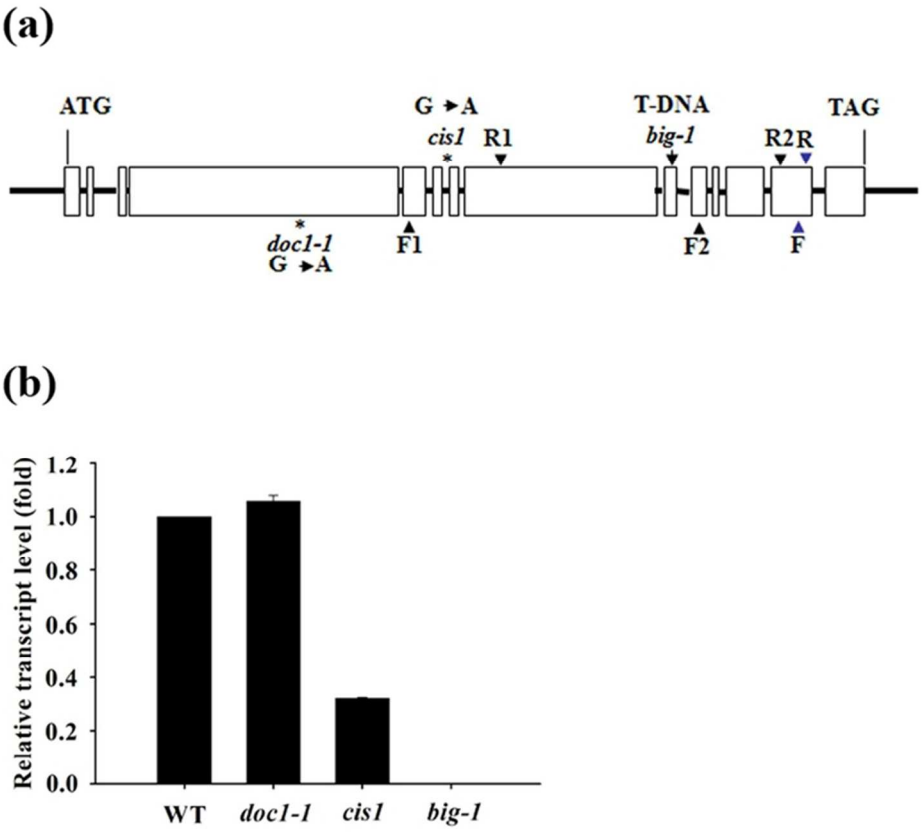

Fig. 2. cis1 is a new allele of the BIG gene.(a) Schematic structure of the BIG gene. The intron and exon organization of the BIG gene shown was determined by comparison of the cDNAs obtained by RT-PCR and genomic sequences from the Arabidopsis WT Col-0. Closed boxes indicate exons, and lines between boxes indicate introns. The locations of the single base mutations and T-DNA insertion of cis1, doc1-1 and big-1 are indicated. Diagram not to scale. (b)The relative mRNA levels of BIG mutant alleles quantified by Q-PCR with a pair primers (F and R) with binding sites shown on (a). Values are mean ± SE, n=3.

71x63mm (300 x 300 DPI)

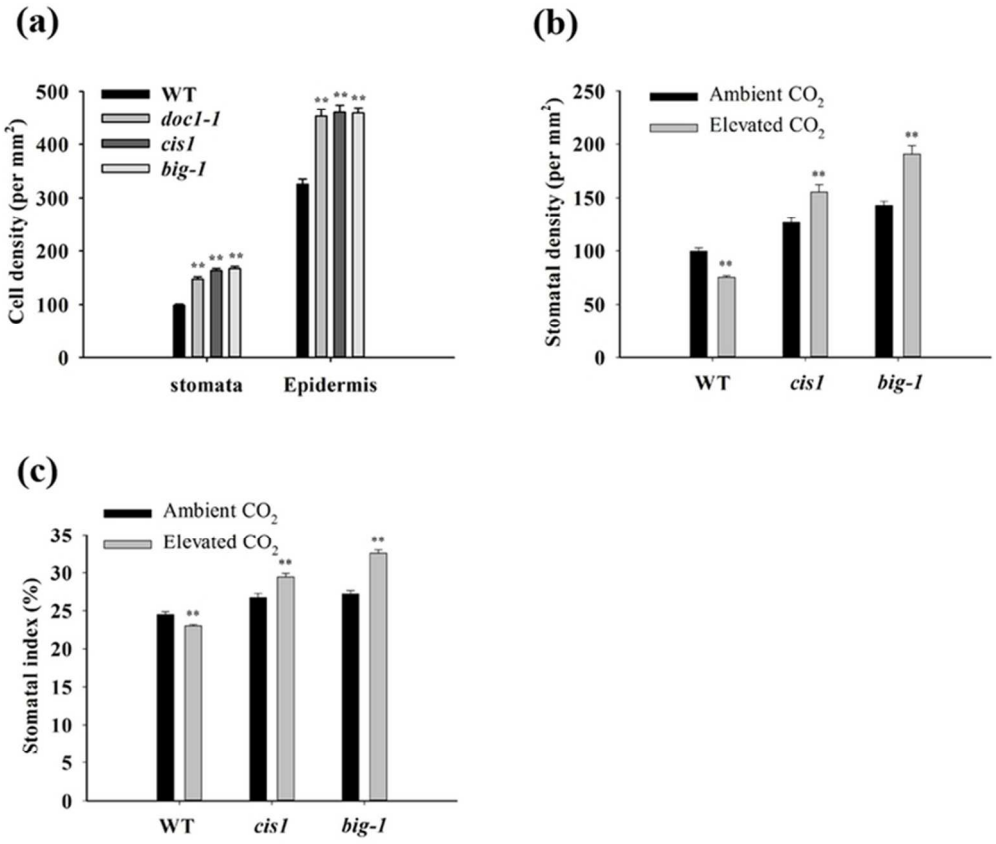

Fig. 3. BIG gene mutants have higher stomatal density than WT. (a) Compared with WT, BIG mutants exhibit increased stomata and epidermal pavement cells (labelled as "Epidermis") density when grown at ambient [CO2]. Error bars represent ± SE (Mann-Whitney rank sum test, **P ≤ 0.001, n=72). (b) Stomatal density of WT and BIG mutant seedlings grown at ambient 450 ppm and elevated 1,000 ppm [CO2]. When grown at 1,000 ppm [CO2] mean stomatal density of WT was significantly reduced compared with growth at ambient [CO2] (Mann-Whitney rank sum test, ** p≤0.001, n>20), whereas in the BIG gene alleles stomatal density increased in these conditions (Student's t test, ** p≤0.001, n>20). (c) Stomatal index of WT and BIG mutant seedlings grown at 450 ppm and 1,000 ppm [CO2]. When grown at 1,000 ppm mean stomatal index of WT was significantly reduced compared with growth at ambient [CO2] (Student's t test, **p≤0.001, n>20), whereas in the BIG gene mutants' stomatal index increased in these conditions (Student's t test, or Mann-Whitney rank sum test, **p≤0.001, n>20).

68x58mm (300 x 300 DPI)

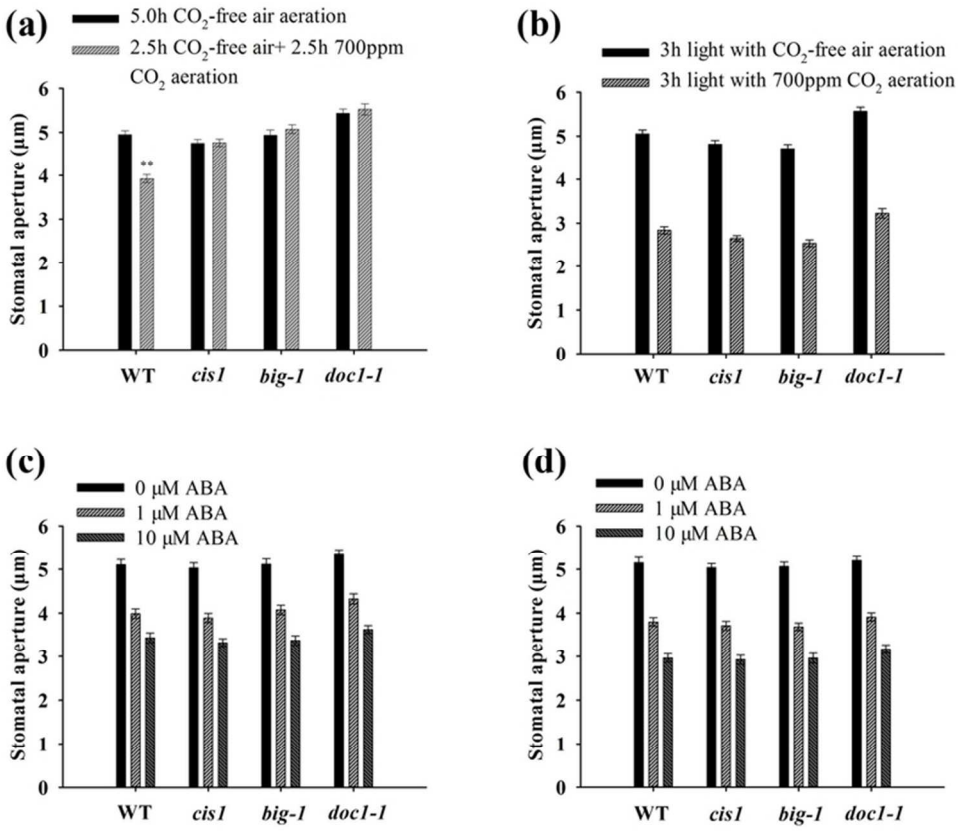

Fig. 4. Stomatal responses of BIG gene mutants to elevated CO2 or exogenous ABA. (a) Elevated CO2-induced stomatal closure is impaired in BIG gene mutants. Values are mean ±SE (Mann-Whitney rank sum test, **P ≤ 0.001, n=40). (b) Elevated CO2 induced inhibition of stomatal opening is not compromised in BIG gene mutants. Error bars represent SE (n=40). (c) ABA-induced stomatal closure is not compromised in BIG gene mutants. Bars=mean ±SE (n=40). (d) The inhibition of light-induced stomatal opening by ABA is not compromised in BIG gene mutants. Values are mean ± SE (n=40).

69x60mm (300 x 300 DPI)

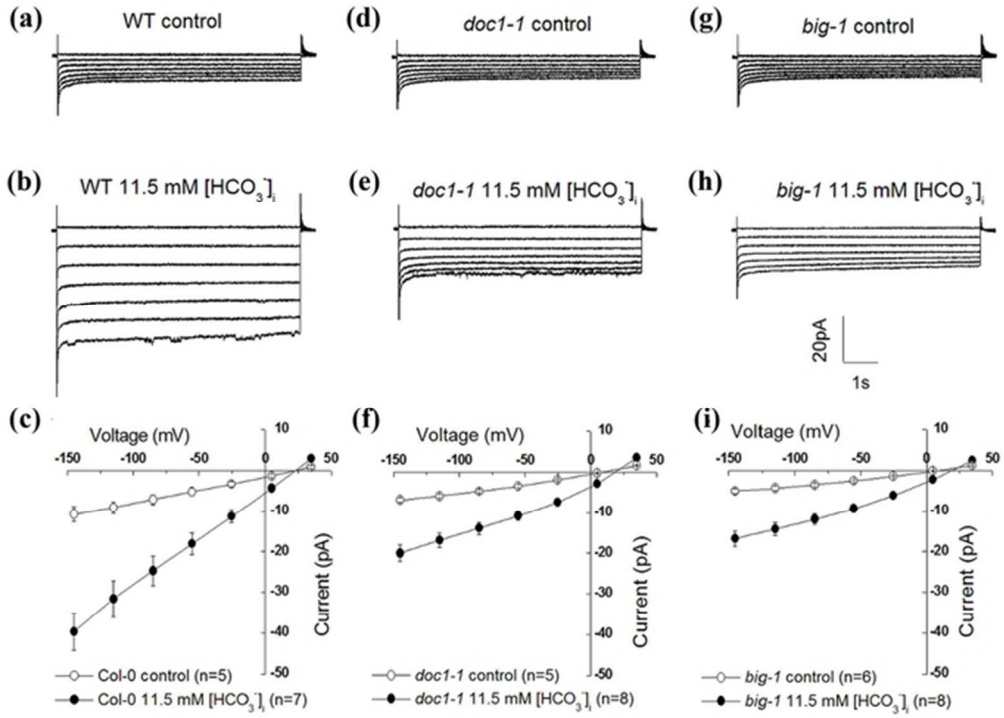

Fig. 5. Bicarbonate-activated S-type anion currents were suppressed in BIG mutant guard cell protoplasts. (a)Typical recording in wild type guard cell protoplasts without bicarbonate. (b)Typical recording of 11.5 mM [HCO3-]i- activated S-type anion currents in wild type guard cell protoplasts. (c) Average current-voltage relationships of whole-cell currents as recording in (a) (open circles, n=5) and (b) (filled circles, n=7). (d) Representative recording in doc1-1 mutant guard cell protoplasts without bicarbonate added in the pipette solution. (e) Representative whole-cell current recording in doc1-1 mutant guard cell protoplasts with 11.5 mM [HCO3-]i added in the pipette solution. (f) Average current-voltage relationships of whole-cell currents as recording in (d) (open circles, n=5) and (e) (filled circles, n=8). (g) Representative recording in big-1 mutant guard cell protoplasts without bicarbonate added in the pipette solution. (h) Representative whole-cell current recording in big-1 mutant guard cell protoplasts with 11.5 mM [HCO3-]i bicarbonate added in the pipette solution. (i) Average current-voltage relationships of whole-cell currents as recording in (g) (open circle, n=6) and (h) (filled circles, n=8).

57x41mm (300 x 300 DPI)